LAB ASTROPHYSICS

Laboratory formation of a scaled protostellar jet by coaligned poloidal magnetic field

B. Albertazzi,[1,2,20] A. Ciardi,[3,4] M. Nakatsutsumi,[1] T. Vinci,[1] J. Béard,[5] R. Bonito,[6,7] J. Billette,[5] M. Borghesi,[8,9] Z. Burkley,[1] S. N. Chen,[1] T. E. Cowan,[10,11] T. Herrmannsdörfer,[11] D. P. Higginson,[1] F. Kroll,[10,11] S. A. Pikuz,[12,13] K. Naughton,[8] L. Romagnani,[1] C. Riconda,[14] G. Revet,[1] R. Riquier,[1,15] H.-P. Schlenvoigt,[11] I. Yu. Skobelev,[12] A.Ya. Faenov,[12,16] A. Soloviev,[17] M. Huarte-Espinosa,[18,19] A. Frank,[18] O. Portugall,[5] H. Pépin,[2] J. Fuchs[1,17]*

Although bipolar jets are seen emerging from a wide variety of astrophysical systems, the issue of their formation and morphology beyond their launching is still under study. Our scaled laboratory experiments, representative of young stellar object outflows, reveal that stable and narrow collimation of the entire flow can result from the presence of a poloidal magnetic field whose strength is consistent with observations. The laboratory plasma becomes focused with an interior cavity. This gives rise to a standing conical shock from which the jet emerges. Following simulations of the process at the full astrophysical scale, we conclude that it can also explain recently discovered x-ray emission features observed in low-density regions at the base of protostellar jets, such as the well-studied jet HH 154.

Narrow bipolar jets are often spectacular and are commonly observed in the universe along the axis of rotation of varied objects, such as young stellar objects (YSOs) surrounded by an accretion disk. Jets are also thought to play a key role in the evolution of these objects. Hence, understanding their formation is key to understanding the mass, energy, and angular momentum redistribution between the dense core and the parent cloud. Once formed, these jets can continue ballistically over large distances (*1*). However, it is important to know how the narrow jet forms and what its characteristics are. The accepted standard model (*2*, *3*) of matter extraction and launching involves a poloidal magnetic field anchored in the disk. Here, poloidal means generally axial with respect to the jet flow, as opposed to the toroidal component that winds around the jet. In the model, matter is magneto-centrifugally accelerated into wide-angle conical winds (*4*). As the magnetic field lines become twisted by the inertia of the initially corotating plasma, the toroidal component of the magnetic field leads to self-collimation of the wind. Nonetheless, this process alone cannot explain collimation of the flow into narrow, jetlike form. First, self-collimation cannot account for the confinement of the whole outflow structure. Indeed, the winds in these models formally extend to infinity and cannot explain the observed jet widths (*5*). Furthermore, jets dominated by a toroidal magnetic field are prone to current and pressure-driven instabilities, which can disrupt the jet (*6*). Efforts to improve the model have led to studies of truncated disk winds where, to collimate the flow, the whole outflow structure has to rely on the thermal pressure of a surrounding medium (*7*), the presence of which has yet to be established.

Alternatively, outflow confinement by a large-scale poloidal magnetic field (*8*) has been explored in numerical simulations (*9*). Although evidence for such fields near the jet source is mostly indirect so far (*10*), they are well established on larger scales (*11*) and observed to be aligned (within ~35°) with the bipolar outflow axes of YSOs. These earlier numerical studies showed that such poloidal fields could convert ejected matter from being weakly collimated to streamlined. However, the simulations lacked a proper treatment of plasma cooling and were constrained by computing limitations to simulate the flow over only small distances from the source. More recently, we revisited the poloidal confinement scenario using large-scale, high-resolution three-dimensional (3D) magneto-hydrodynamic (MHD) simulations (*12*), which included cooling, and we showed that the whole outflow could be constrained. Notably, we predicted a particular morphology for the outflow with a shock-bounded cavity followed by a narrow jet. Such a mechanism does not exclude magneto-centrifugal self-collimation: Even if poloidal collimation can act on its own, it can also be complementary to self-collimation by stabilizing and further collimating the jets produced by the latter.

We report here on scaled laboratory experiments that exploit coupling of a high-amplitude and large-scale magnetic field to high-velocity plasma flows, to create conditions representative of a YSO. Our measurements conclusively demonstrate that stable jets can indeed be collimated from a wide-angle star/disk wind embedded in a coaligned, large-scale poloidal magnetic field. This is notably obtained without having to rely on the collimation by an external medium. We also show that the stable collimation of the whole flow into a narrow jet can be obtained even in the case of an angular offset (up to 40°) between the magnetic field and the outflow axis. The transition (Fig. 1A) from a divergent to a narrowly collimated flow results from the plasma being redirected toward the axis by a shock structure, which is induced by the compression of the magnetic field lines under the action of the expanding plasma. Consequently, a standing conical shock feature forms at the converging point where the plasma becomes reheated. We performed full-scale astrophysical simulations of an isotropic wind embedded in a large-scale magnetic field under conditions typical of YSOs, which appear consistent with the laboratory observations. By calculating the x-ray emission from the simulated plasma, we determine that the shock-focused region generates an x-ray source whose luminosity and location are in agreement with the Chandra observations of the puzzling x-ray emission from HH 154, one of the best-studied astrophysical jets emerging from a YSO (*13*).

The laboratory plasma, mimicking a YSO flow, is produced by short (0.5-ns), high-power laser irradiation of massive solid (plastic) targets (see methods). The plasma is a highly conductive and superfast-magnetosonic flow. The plasma is thermally launched from a region on the target on the order of the laser spot diameter (0.75 mm), and this wide-angle flow is, as it is in a YSO, initially dominated by its kinetic energy. The scaling between the laboratory plasma and a YSO outflow allows us also to scale a time span of 20 ns

[1]Laboratoire d'Utilisation des Lasers Intenses (LULI), École Polytechnique, CNRS, Commissariat à l'Energie atomique et aux énergies alternatives (CEA), Université Pierre et Marie Curie (UPMC), F-91128 Palaiseau, France. [2]Institut National de la Recherche Scientifique–Energie, Matériaux, Télécommunications (INRS-EMT), Varennes, Québec, Canada. [3]Sorbonne Universités, UPMC Université. Paris 06, UMR 8112, Laboratoire d'Etudes du Rayonnement et de la Matière en Astrophysique (LERMA), F-75005 Paris, France. [4]Observatoire de Paris and CNRS, UMR 8112, LERMA, Paris, France. [5]Laboratoire National des Champs magnétiques Intenses (LNCMI), UPR 3228, CNRS-Université Joseph Fourier (UJF)-Université Paul Sabatier (UPS)-Institut National des Sciences Appliquées (INSA), F-31400 Toulouse, France. [6]Dipartimento di Fisica e Chimica, Università di Palermo, Piazza del Parlamento, I-1 90134 Palermo, Italy. [7]National Institute for Astrophysics (INAF)–Osservatorio Astronomico di Palermo, Piazza del Parlamento, I-1 90134 Palermo, Italy. [8]School of Mathematics and Physics, The Queen's University of Belfast, Belfast BT7 1NN, UK. [9]Institute of Physics of the Academy of Science of the Czech Republic (ASCR), Extreme Light Infrastructure (ELI)-Beamlines Project, Na Slovance 2, 18221 Prague, Czech Republic. [10]Technische Universität Dresden, D-01062 Dresden, Germany. [11]Helmholtz-Zentrum Dresden-Rossendorf, Bautzner Landstrasse 400, D-01328 Dresden, Germany. [12]Joint Institute for High Temperatures Russian Academy of Science (RAS), Moscow 125412, Russia. [13]National Research Nuclear University MEPhI, Moscow 115409, Russia. [14]Sorbonne Universités, UPMC Université Paris 06, UMR 7605, LULI, F-75005 Paris, France. [15]CEA–Bruyères le Chatel, F-91297 Arpajon, France. [16]Institute for Academic Initiatives, Osaka University, Suita, Osaka 565-0871, Japan. [17]Institute of Applied Physics, 46 Ulyanov Street, 603950 Nizhny Novgorod, Russia. [18]Department of Physics and Astronomy, University of Rochester, Rochester, NY, USA. [19]Center for Advanced Computing and Data Systems, University of Houston, Houston, TX 77204, USA. [20]Graduate School of Engineering, Osaka University, Suita 565-0871, Japan.
*Corresponding author. E-mail: julien.fuchs@polytechnique.fr

in the laboratory to an equivalent ~6 years in the natural environment, during which it propagates over ~600 astronomical units (AU). Hence, even over short time scales (<100 ns), the experiment has the ability to sample the stationary morphology of an astrophysical outflow. Toroidal magnetic fields, which are self-generated in the plasma outflow owing to crossed density and temperature gradients (*14*), have a low amplitude in our study, because of the low laser intensity that we used (see methods). At the same time, they are limited to zones close (<0.5 mm) to the target surface and thus are not able to confine the flow beyond that (Fig. 1D): The plasma then freely expands at a wide angle. In short, this experimental configuration mimics well the expansion of one hemisphere of a naturally occurring YSO spherical wind that emerges at large distances from the disk, where acceleration is complete and gravitational effects are unimportant.

A steady (i.e., with duration >5 μs) and homogeneous axial magnetic field can be applied to the laboratory plasma (see methods). The magnetic field extends over a large volume (3 cm in length and 1 cm in diameter) with a strength of up to 0.4 MG (*15*). The plasma flow in this case is well approximated by ideal MHD (*16*), ensuring its relevance as a scaled astrophysical plasma. Indeed, the dimensionless Reynolds (*Re*), magnetic Reynolds (*ReM*), and Peclet (*Pe*) numbers are much larger than unity ($Re \sim 10^4$ to 10^5; *ReM* ~50; *Pe* ~ 3 to 5). This implies that the advective transport of momentum, magnetic field, and thermal energy dominates over diffusive transport, as expected in a YSO outflow. The strength of the magnetic field in which the plasma is embedded is much larger than in the astrophysical environment (on the order of milligauss) (*10*), to compensate for the shortness of the space and the time scales of the experiment. This means that the ratio of the plasma's kinetic ram pressure to magnetic pressure will transition from >>1 to <<1 over a few millimeters, while it does the same over a few tens of astronomical units in a YSO.

The typical morphology of our laboratory plasma, when applying the axial magnetic field to it, is shown in Fig. 1B. We present a measurement of the integrated electron density along the line of sight of the expanding plasma obtained through transverse optical laser probing. The axial magnetic field has a profound effect on the collimation of the laser-produced plasma flow, thus leading to the emergence of a narrow jet with an aspect ratio of >10 that is maintained over the entire homogeneous magnetic field region with little variation in density. Such tight collimation is also observed when imaging the x-ray emission in the kilo–electronvolt range originating from the plasma (see methods) and is in excellent agreement with our earlier MHD numerical investigations (*12*). We emphasize that even laser experiments specifically designed to produce jets from radiatively cooled, unmagnetized plasmas do not exhibit such morphology and have in fact much lower aspect ratios (*17*–*19*). The mechanism leading to the tight magnetic collimation of the plasma plume is illustrated in Fig. 1, C and D. We also present 3D resistive MHD numerical simulations using the parameters of the experiment (Fig. 2; see methods). When the laboratory plasma expands in the presence of a magnetic field (Fig. 1C), one clearly observes the formation of a converging cavity with an outer shell of higher electron density. We stress that neither the cavity nor the jet is observed when no magnetic field is applied (Fig. 1D). The formation of this shell is the consequence of the accumulation and heating of

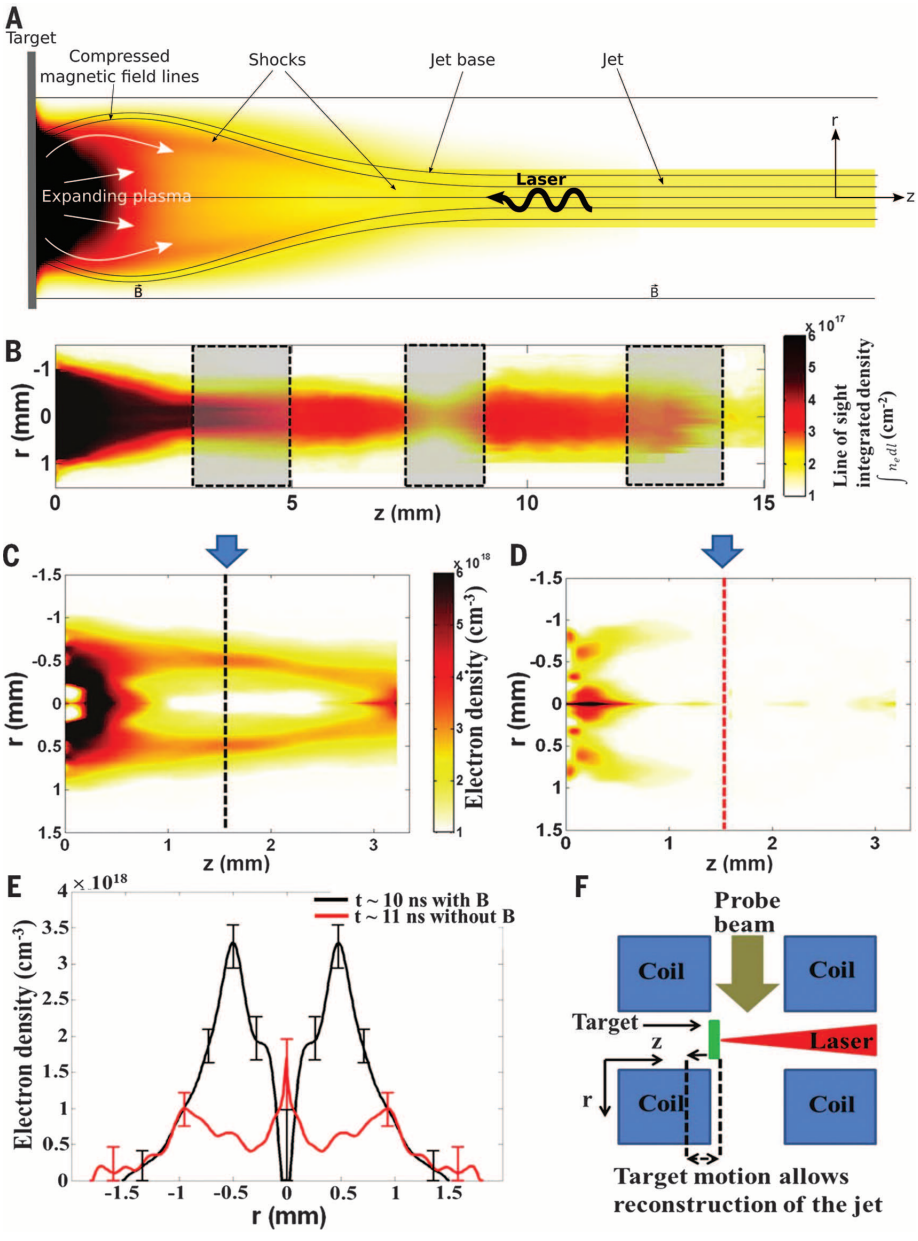

Fig. 1. Laboratory demonstration of jet formation by axial magnetic field. (**A**) Cartoon of the experiment and of the jet-formation mechanism. (**B**) Integrated plasma density measured 20 ns after the laser irradiation (from the right) of a plastic (CH) target (left) immersed in the *z*-oriented [see (A)] 0.2-MG magnetic field. Four images obtained with different target positions are used [see (F)]. Shaded areas indicate linear interpolation in between observed sections of the jet (in the middle section, flow gradients, converging on the left and diverging on the right, indicate the presence of a refocusing intermediate point). (**C** and **D**) Abel inverted density maps (the color map applies to both images) with (C) and without (D) a magnetic field; and (**E**) profiles [along the dashed lines shown in (C) and (D)] show the cavity region, and plasma convergence on-axis that is induced by the magnetic field. The error bars in (E) represent the difference in the plasma density retrieved by Abel inversion from the upper and lower measured phase maps (see methods). (**F**) Target and magnetic field arrangement used in the experiment.

plasma in a fast-mode oblique shock generated by the external magnetic field halting the radial expansion of the flow. Because the plasma is of high temperature and has a superfast-magnetosonic expansion speed (200 to 500 km/s, similar to the outflow velocity measured in YSO), the magnetic field lines are bent and compressed past this shocked envelope (Fig. 2).

The expanding plasma from the target is refracted across this oblique shock and slides along the walls of the cavity, which has been curved toward the axis by the magnetic forces. When the flow reaches a convergence point, it stagnates and forms a conical shock, which focuses the flow along the polar axis and generates a narrow jet ahead of the convergence point. This convergence of plasma toward the axis (at z ~3 mm) is visible in the experimental images (Fig. 1, B and C), and our simulations reveal that the plasma becomes heated to ~70 eV by this shock. When applying the external magnetic field, substantial plasma heating (compared to what is observed in the freely expanding plasma) is also seen by our spectrally resolved diagnostic that images the x-ray emission (see methods) (*20*). This mechanism of jet formation is similar to astrophysical models of hydrodynamic collimation of a wind by the inertia of a dense, torus-like circumstellar envelope (*21*). However, we demonstrate here that it can operate even in the absence of a surrounding medium.

The overall jet-formation process illustrated here for a particular set of laser and target conditions was repeatable and effective over a wide variety of different experimental conditions. The jets were always found to be in agreement with MHD modeling, hence validating the physical mechanism described above. Notably, when the laser intensity on the target was increased, we could increase the kinetic pressure at the target surface. This produced a wider cavity and moved the shock convergence region further away along the jet axis. Similarly, we could also move the distance of the shock with respect to the plasma source by varying the magnetic field strength. Contrary to what takes place in the experiment, if the deposition of energy was continuous, the location of the shock convergence region of the jet would be stationary. Finally, when we tilted the target and likewise the axis of the plasma expansion with respect to the magnetic field axis, we still observed the cavity formation and plasma focusing on-axis, even for angular offsets up to 40°, showing that the mechanism is robust.

We find the same morphology of the wind tightly focusing into a convergence point and forming a jet in the same direction in full-scale

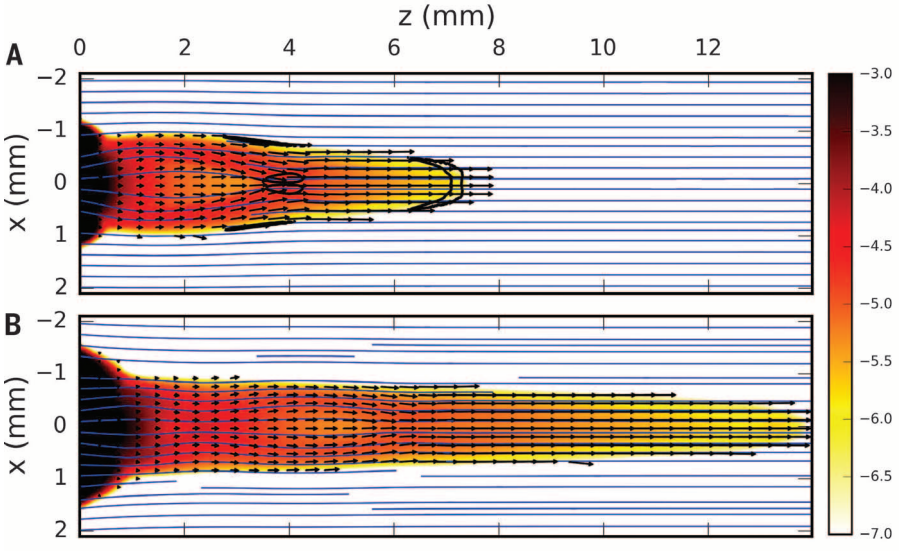

Fig. 2. Three-dimensional MHD modeling of the experiment. The maps show two snapshots [(**A**) 10 ns and (**B**) 20 ns from the end of the laser pulse] of the density ($\log_{10}$ ρ in g cm^{-3}) of the carbon plasma along the *x*-*z* plane. The arrows represent velocity vectors, and the lines represent the magnetic field. The black contour line shows plasma heated to a temperature above 70 eV.

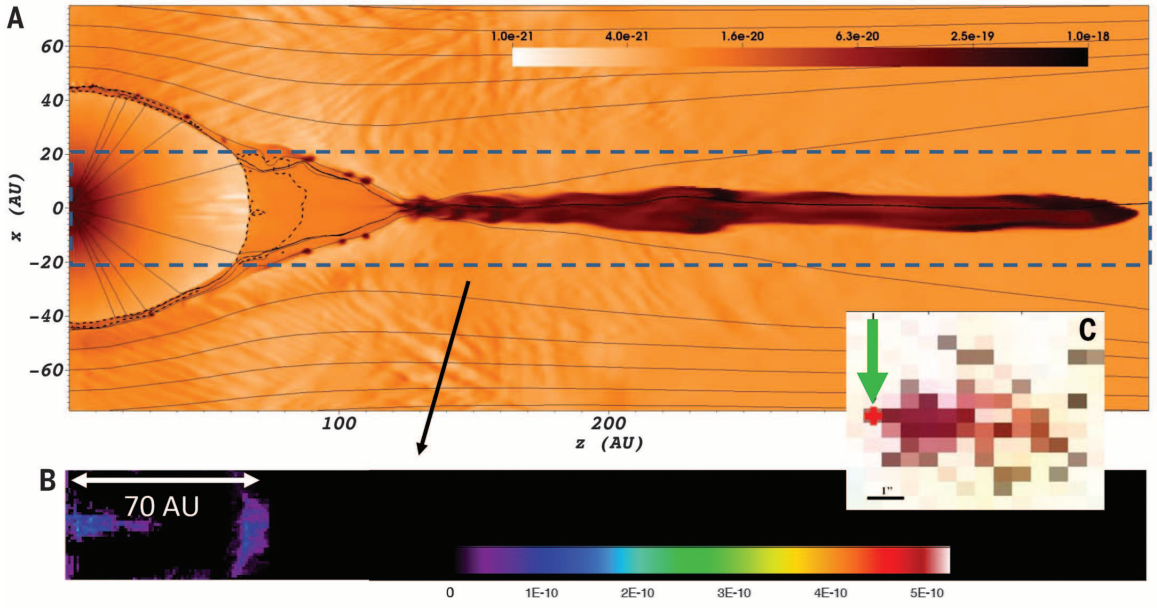

Fig. 3. Three-dimensional simulation of jet formation and collimation in a young star system embedded in a 5-mG axial magnetic field. An isotropic wind of H from the combined star–disk system with a mass ejection rate of 10^{-8} $M_\odot$/year and velocity 200 km/s is embedded in an initially axial (z) magnetic field. (**A**) (*x*-*z*) mass density ($\log_{10}$ ρ in g cm^{-3}) at time 20 years. Black lines: magnetic field lines; dashed contour: plasma of temperature ≥70 eV. (**B**) X-ray emission synthesized (see methods) from the simulated plasma of (A) (counts/s in each pixel with size of 1 AU). (**C**) X-ray emission image of HH154 as detected by the Chandra telescope. The color map ranges from white (no emission) to red. The stationary emission feature that is the brightest zone in the image, and that is located ~60 to 80 AU away from the star (located by the red dot at the tip of the green arrow), has a luminosity and a distance to the source that is consistent with the simulated bright region located at 70 AU in (B).

astrophysical simulations (Fig. 3A; see methods), performed with mass-ejection rates (*22*) and magnetic field strengths (*10*) typical of YSOs. We further verified that the range of density and temperature conditions found along the jet implies that the material within covers the full range of ionization fraction, with most of the jet part being only weakly ionized, consistent with observations (*23*). We see the principal dynamics and features of the laboratory flows also in the simulation results, which support the scalability of the laboratory experiment. We varied the wind and field parameters extensively with detailed numerical simulations to verify that the poloidal-field–induced jet collimation mechanism was a very robust process.

An interesting outcome of our study is that typical YSOs should then have a stationary region of shock-heated plasma that forms within a few tens to 100 AU from the wind source (see Fig. 3A). This numerical prediction can be directly compared to the analysis of observations made over more than one decade using x-ray satellites that have revealed (see Fig. 3C) bright sources of stationary x-ray emission zones located at the base of jets (~100 AU from the source) emerging from a YSO (*24*–*26*) and distinct from it. They have not been explained so far by self-collimation models of jet formation but are still consistent with the process revealed here (Fig. 3B).

We have therefore proposed a simple and plausible scenario for the collimation of a narrow stable jet past its launching phase (*1*, *2*) that is consistent with recent astrophysical observations (*10*, *24*, *25*). In addition to helping to advance the understanding of jet–core interaction in YSOs, our work enables studying and/or modeling important aspects of jet physics in the laboratory. These include, e.g., transverse instabilities that can affect the jet structure, or episodic ejections, i.e., multicomponent and time-dependent interacting winds, which can be easily simulated in the laboratory by using multiple laser pulses separated by a few nanoseconds. Producing such magnetized narrow plasma columns and letting them strike a solid will also uniquely allow the study of plasma dynamics in accretion columns in young stars; that is, one can model magnetic arches that are loaded with disk material that free-falls toward the star. Beyond these aspects, adapting the present experimental work to other configurations will permit advances in resolving pending questions about a wide range of astrophysical and plasma physics systems where magnetic fields are thought to play an important role.

REFERENCES AND NOTES

1. A. Frank, T. P. Ray, S. Cabrit, P. Hartigan, H. G. Arce, F. Bacciotti, J. Bally, M. Benisty, J. Eislöffel, M. Güdel, S. Lebedev, B. Nisini, A. Raga, *Jets and Outflows From Star to Cloud: Observations Confront Theory, in Protostars and Planets VI*, H. Beuther, R. Klessen, C. Dullemond, Th. Henning, Eds. (Univ. of Arizona Press, Tucson, 2014).
2. R. D. Blandford, D. G. Payne, *Mon. Not. R. Astron. Soc.* **199**, 883–903 (1982).
3. J. Ferreira, *Astron. Astrophys.* **319**, 340–359 (1997).
4. R. E. Ainsworth, T. P. Ray, A. M. M. Scaife, J. S. Greaves, R. J. Beswick, *Mon. Not. R. Astron. Soc.* **436**, L64–L68 (2013).
5. M. Stute, J. Gracia, K. Tsinganos, N. Vlahakis, *Astron. Astrophys.* **516**, A6 (2010).
6. R. Moll, H. C. Spruit, M. Obergaulinger, *Astron. Astrophys.* **492**, 621–630 (2008).
7. T. Matsakos *et al.*, *Astron. Astrophys.* **502**, 217–229 (2009).
8. H. C. Spruit, T. Foglizzo, R. Stehle, *Mon. Not. R. Astron. Soc.* **288**, 333–342 (1997).
9. S. Matt, R. Winglee, K.-H. Böhm, *Mon. Not. R. Astron. Soc.* **345**, 660–670 (2003).
10. P. Hartigan, A. Frank, P. Varniére, E. G. Blackman, *Astrophys. J.* **661**, 910–918 (2007).
11. N. L. Chapman *et al.*, *Astrophys. J.* **770**, 151 (2013).
12. A. Ciardi *et al.*, *Phys. Rev. Lett.* **110**, 025002 (2013).
13. F. Favata *et al.*, *Astron. Astrophys.* **450**, L17–L20 (2006).
14. J. A. Stamper, *Laser Part. Beams* **9**, 841–862 (1991).
15. B. Albertazzi *et al.*, *Rev. Sci. Instrum.* **84**, 043505 (2013).
16. D. D. Ryutov, R. P. Drake, B. A. Remington, *Astrophys. J. Suppl. Ser.* **127**, 465–468 (2000).
17. D. Farley *et al.*, *Phys. Rev. Lett.* **83**, 1982–1985 (1999).
18. B. Loupias *et al.*, *Phys. Rev. Lett.* **99**, 265001 (2007).
19. Ph. Nicolaï *et al.*, *Phys. Plasmas* **15**, 082701 (2008).
20. A. Faenov *et al.*, *Phys. Scr.* **53**, 591–596 (1996).
21. B. Balick, A. Frank, *Annu. Rev. Astron. Astrophys.* **40**, 439–486 (2002).
22. S. Cabrit, in *Star-Disk Interaction in Young Stars*, Proceedings IAU Symp. no. 243, J. Bouvier, I. Appenzeller, Eds. (Cambridge Univ. Press, Cambridge, 2007), pp. 203–214.
23. L. Maurri *et al.*, *Astron. Astrophys.* **565**, A110 (2014).
24. M. Güdel, S. L. Skinner, M. Audard, K. R. Briggs, S. Cabrit, *Astron. Astrophys.* **478**, 797–807 (2008).
25. P. C. Schneider, H. M. Günther, J. H. M. M. Schmitt, *Astron. Astrophys.* **530**, A123 (2011).
26. R. Bonito *et al.*, *Astrophys. J.* **737**, 54 (2011).

ACKNOWLEDGMENTS

We acknowledge the support of the LULI teams and of S. Dittrich and S. Nitsche (Helmholtz–Zentrum Dresden–Rossendorf) and discussions with P. Audebert. This work was supported by grant E1127 from Région Ile-de-France, Agence Nationale de la recherche (ANR) white grant 12-BS09-025-01 SILAMPA, grant ELAM from Réseau thématique de recherche avancé (RTRA)-Saclay, a grant from RTRA–Triangle de la Physique, grants Engineering and Physical Sciences Research Council (EPSRC) EP/I029206/1 and EP/J500094/1, and the Natural Sciences and Engineering Research Council of Canada (NSERC) Discovery grant 26558-2007 RGPIN. This work was partly done within the LABEX Plas@Par project and received financial state aid managed by the Agence Nationale de la Recherche, as part of the program "Investissements d'avenir" under the reference ANR-11-IDEX-0004-02. This work was supported in part by the Ministry of Education and Science of the Russian Federation under contract no. 14.Z50.31.0007. S.N.C. acknowledges the support received during this work by NSF grant 1064468. Experimental data and simulations are, respectively, archived on servers at LULI and LERMA laboratories and can be consulted upon demand. Part of the experimental system is covered by a patent (1000183285, 2013, Institut National de la Propriété Industrielle–France).

SUPPLEMENTARY MATERIALS

www.sciencemag.org/content/346/6207/325/suppl/DC1
Materials and Methods
References (*27*–*32*)

6 August 2014; accepted 17 September 2014
10.1126/science.1259694

OPTICS

Loss-induced suppression and revival of lasing

B. Peng,[1]* Ş. K. Özdemir,[1]*† S. Rotter,[2] H. Yilmaz,[1] M. Liertzer,[2] F. Monifi,[1] C. M. Bender,[3] F. Nori,[4,5] L. Yang[1]†

Controlling and reversing the effects of loss are major challenges in optical systems. For lasers, losses need to be overcome by a sufficient amount of gain to reach the lasing threshold. In this work, we show how to turn losses into gain by steering the parameters of a system to the vicinity of an exceptional point (EP), which occurs when the eigenvalues and the corresponding eigenstates of a system coalesce. In our system of coupled microresonators, EPs are manifested as the loss-induced suppression and revival of lasing. Below a critical value, adding loss annihilates an existing Raman laser. Beyond this critical threshold, lasing recovers despite the increasing loss, in stark contrast to what would be expected from conventional laser theory. Our results exemplify the counterintuitive features of EPs and present an innovative method for reversing the effect of loss.

Dissipation is ubiquitous in nature; the states of essentially all physical systems thus have a finite decay time. A proper description of this situation requires a departure from conventional Hermitian models with real eigenvalues and orthogonal eigenstates to non-Hermitian models featuring complex eigenvalues and nonorthogonal eigenstates (*1*–*3*). When tuning the parameters of such a dissipative system, its complex eigenvalues and the corresponding eigenstates may coalesce, giving rise to a non-Hermitian degeneracy, also called an exceptional point (EP) (*4*). The presence of such an EP has a dramatic effect on the system, leading to nontrivial physics with interesting counterintuitive features such as resonance trapping (*5*), a mode exchange when encircling an EP (*6*), and a singular topology in the parameter landscape (*7*). These characteristics can control the flow of light in optical devices with both loss and gain. In particular, waveguides with parity-time symmetry (*8*), where loss and gain are balanced, have attracted enormous attention (*9*, *10*), with effects

[1]Department of Electrical and Systems Engineering, Washington University, St. Louis, MO 63130, USA. [2]Institute for Theoretical Physics, Vienna University of Technology, A-1040 Vienna, Austria. [3]Department of Physics, Washington University, St. Louis, MO 63130, USA. [4]Center for Emergent Matter Science, RIKEN, Wako-shi, Saitama 351-0198, Japan. [5]Department of Physics, University of Michigan, Ann Arbor, MI 48109, USA.
*These authors contributed equally to this work. **†Corresponding author. E-mail: ozdemir@ese.wustl.edu (S.K.O.); yang@ese.wustl.edu (L.Y.)**

Laboratory formation of a scaled protostellar jet by coaligned poloidal magnetic field

B. Albertazzi, A. Ciardi, M. Nakatsutsumi, T. Vinci, J. Béard, R. Bonito, J. Billette, M. Borghesi, Z. Burkley, S. N. Chen, T. E. Cowan, T. Herrmannsdörfer, D. P. Higginson, F. Kroll, S. A. Pikuz, K. Naughton, L. Romagnani, C. Riconda, G. Revet, R. Riquier, H.-P. Schlenvoigt, I. Yu. Skobelev, A.Ya. Faenov, A. Soloviev, M. Huarte-Espinosa, A. Frank, O. Portugall, H. Pépin and J. Fuchs

Science **346** (6207), 325-328.
DOI: 10.1126/science.1259694

Stellar outflows replicated in miniature

Astronomers observe tight bright jets beaming from the poles of many celestial objects. But what focuses them so well? Albertazzi *et al.* recreated a scaled-down plasma jet in a laboratory setting to match the behavior of those in young stellar objects. The experiments show that the jets are collimated by a poloidal magnetic field aligned with the same axis. A conelike shock also emerges, as the expanding plasma is abruptly confined by the magnetic field.

Science, this issue p. 325